Available online at www.sciencedirect.com
SCIENCE DIRECT®
Journal of Nuclear Materials 337–339 (2005) 776–780
journal of nuclear materials
www.elsevier.com/locate/jnucmat

Influence of ELMs on operation of ICRF antennas in ASDEX Upgrade

Vl.V. Bobkov [a,*], F. Braun [a], D.A. Hartmann [a], P. Lamalle [b], I. Monakhov [c], J.-M. Noterdaeme [a,d], P. Wouters [b], E. Würsching [a], ASDEX Upgrade Team

[a] *Max-Planck-Institute fuer Plasmaphysik, Boltzmannstr. 2, D-85748 Garching, Germany*
[b] *LPP-ERM/KMS, Association EURATOM-Belgian State, TEC, Royal Military Academy, B-1000 Brussels, Belgium*
[c] *EURATOM/UKAEA Fusion Association, Culham Science Centre, Abingdon OX14 3DB, UK*
[d] *EESA Department, Gent University, B-9000 Gent, Belgium*

Abstract

The coupling characteristics of the ion cyclotron range of frequencies antenna during type I edge localized modes (ELMs), asymmetries in the reaction of toroidally distributed antennas to ELMs and arcing phenomena following ELMs are studied for ASDEX Upgrade. The maximum change of the antenna resistance due to ELMs increases with triangularity δ_L in the on-axis minority heating. In the cases with off-axis heating, the change of the resistance is less sensitive to δ_L. Time-resolved RF measurements show asymmetries in times of response of the toroidally distributed antennas to the rising edge of ELMs and in the further evolution of this response. Toroidal propagation of ELM perturbations in counter-current direction with times $\approx 50\,\mu s$ for one toroidal turn is observed. ELM-induced arcing is observed during ELMs and with delays after ELMs. Conditioning takes place as the arc number during ELMs decreases and time delay between ELM and arc increases.

PACS: 52.50.G; 52.40.F; 52.40.H; 51.50
Keywords: ASDEX Upgrade; ELM; ICRF antenna; RF discharge

1. Introduction

Detailed understanding of the properties of ICRF (Ion Cyclotron Range of Frequencies) antennas in type I ELMy discharges, and during ELMs in particular, is essential for designing ITER relevant ICRF systems that are able to cope with ELMs. ELMs lead to a significant change of the plasma density in front of the ICRF antennas. This influences the position of the cut-off of the fast waves used for plasma heating, affects parasitic absorption of the RF power at the plasma boundary [1] and influences voltage stand-off [2]. The following aspects of the operation of the antennas in ELMy plasma are studied:

- coupling characteristics of a single antenna or antenna strap and dependencies on plasma parameters – to provide information to design an ELM-resilient RF system;

* Corresponding author. Tel.: +49 89 32991869; fax: +49 89 32992558.
E-mail address: volodymyr.bobkov@ipp.mpg.de (Vl.V. Bobkov).

0022-3115/$ - see front matter © 2004 Elsevier B.V. All rights reserved.
doi:10.1016/j.jnucmat.2004.10.109

- asymmetries of reaction of different antennas/straps – many ELM-resilient systems are based on connection of two antennas/straps together in a RF compensation scheme [3–6];
- ELM-induced RF arcing inside the antennas [2] – various mechanisms of high voltage breakdown exist in the presence of the plasma delivered to the antennas during ELMs and may lead to an unexpected reaction of safety circuits and affect conditioning.

On the other hand, besides plasma heating, ICRF antennas may provide useful information on ELM physics acting as a diagnostic for ICRF-heated discharges (e.g. [7]).

2. ICRF antennas at ASDEX Upgrade and RF measurements

ASDEX Upgrade (AUG) has four ICRF antennas located at the low field side, each antenna consisting of two straps [8]. The antenna straps are connected to resonant lines with 25 Ω characteristic impedance ('strap resonant lines') which are then connected via a T to the matching circuit (two stub tuners). The use of 3 dB hybrid couplers [6] allows to have low levels of reflected powers at RF generators during AUG discharges, including discharges with type I ELMs. Measurements of coupling characteristics and asymmetries were conducted at 30 MHz.

To calculate the antenna strap resistance during ELMs, the measurement of maximal voltage in the resonant line of one strap is combined with the measurements of the forward and reflected powers in the matched line. It is assumed that the net power is the same for each of the two straps of the antenna, i.e. each strap takes half of the power delivered to the antenna. Phase measurements were performed using two directional couplers in the strap resonant line. RF voltage and current were measured for all antennas at the strap resonant lines about ≈2.5 m away from the antenna feeders in order to compare the response of the antennas to ELMs. The voltage and current probes are located between RF voltage maximum and RF current maximum, closer to the latter. Voltage to current ratio is used to characterize structure of the asymmetry. The signals of RF currents decrease rapidly during ELMs; they were used to infer the time delays of the response of the coupling of the different antennas to ELMs.

To confirm arcing events inside an antenna, the reflected powers from two antennas are compared. If the powers deviate from each other significantly, it is assumed that an arc occurred in the antenna with the higher reflected power.

3. Experimental results

3.1. Coupling characteristics of antenna during ELMs

The change of the antenna resistance during ELMs depend on many parameters: plasma density profile, plasma shape (triangularity and antenna–plasma distance), ELM particle losses, etc. To characterize ELM particle losses, a detailed approach is often applied (e.g. [9]) including evaluation of density and temperature profiles. In our (more simple) analysis ELMs are detected from H_α signal from the outer divertor. As the

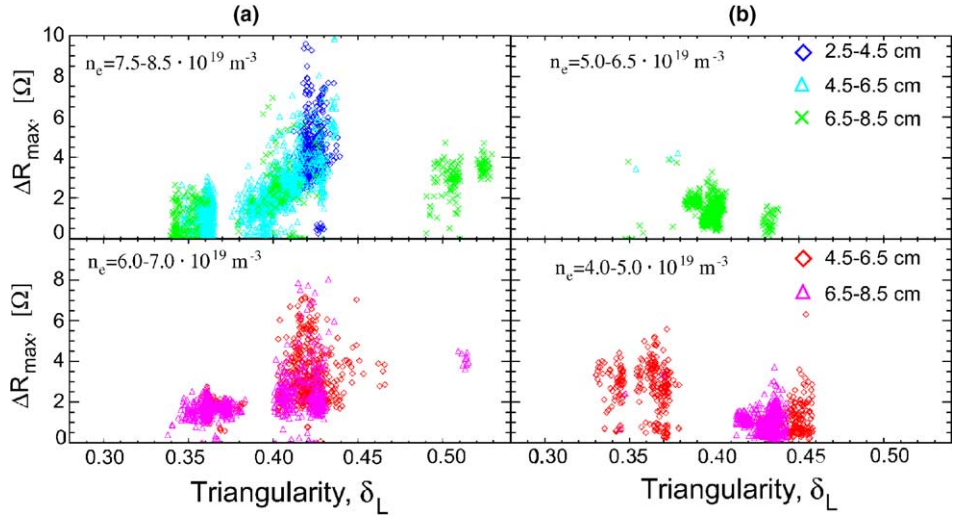

Fig. 1. Change of the antenna resistance depending on the lower triangularity for fixed line-averaged density and averaged antenna–plasma distance: (a) on-axis ICR heating, (b) extreme off-axis ICR heating.

most crucial parameters which affect changes of the antenna resistance during ELMs, we note: central line-averaged density, plasma triangularity (lower) δ_L and averaged antenna–plasma distance (average of the distances between plasma and the antenna poloidal limiter at the top, at the middle and at the bottom of the antenna).

Fig. 1 presents results of the analysis of 54 plasma discharges with type I ELMs and hydrogen minority ICRF heating in deuterium with the launched power in the range 1.5–5 MW. The figure illustrates a dependence of the maximal change of the antenna resistance during ELMs on the plasma triangularity for on-axis heating (Fig. 1(a)) and off-axis heating, when the cyclotron resonance of hydrogen minority is placed at a distance of ≈10–20 cm from the antenna (Fig. 1(b)). In both cases similar amplitudes of H_α signals were observed.

One observes that for a fixed line-averaged density and averaged antenna–plasma distance, the change of the resistance grows when the triangularity increases in discharges with on-axis minority heating. The same kind of dependence is observed at JET and reported in [10]. The phase measurements for the on-axis heating also show the same behaviour as at JET: change of the effective length of the antennas is negative during ELMs and has higher amplitude at high triangularity. In a particular case, the change of the effective length of the AUG antenna due to an ELM was measured to be ≈3 cm at low triangularity and ≈35 cm at high triangularity.

During off-axis minority heating at AUG, the change of the antenna resistance is not so sensitive to the triangularity and even becomes smaller when triangularity is increased. No measurements of effective electrical length of the antennas have been conducted for the off-axis heating.

3.2. Toroidal asymmetry and propagation of ELM perturbation

RF antennas react sensitively on the density change in front of them (in the outer scrape-off-layer). During the beginning of ELMs, the density profile in front of the antennas is highly irregular in three dimensions, since ELM is characterized as a number of helical plasma filaments, elongated along magnetic field lines. If structure of the filaments is not stationary in time with respect to the ICRF antennas, the antennas response can have a unique time evolution for each antenna. In Fig. 2(a), V/I ratios in the resonant line of each strap of the four antennas are shown together with H_α time trace for a type I ELM in a discharge with $\delta_L = 0.4$ and central line-averaged density $6 \times 10^{19}\,m^{-3}$. The loss of diamagnetic energy for this ELM is ≈30 kJ (≈4.5%), i.e. it can be characterized as a 'strong' type I ELM at AUG. One observes that in the first ≈500 μs of the ELM, a highly structured pattern of the time traces is recognizable. The pattern is very similar for adjacent straps within one antenna and for adjacent antennas, and is significantly different for the antennas located opposite to each other in the torus. After the 500 μs time, the time traces become smooth and similar for all antenna straps indicating that the density profile in front of the antennas has no three dimensional peculiarities changing in time with respect to the antennas. During the latter phase, when the density profile in front of the antennas is smooth and monotonic, the antenna coupling can be successfully modeled by numerical calculations [7].

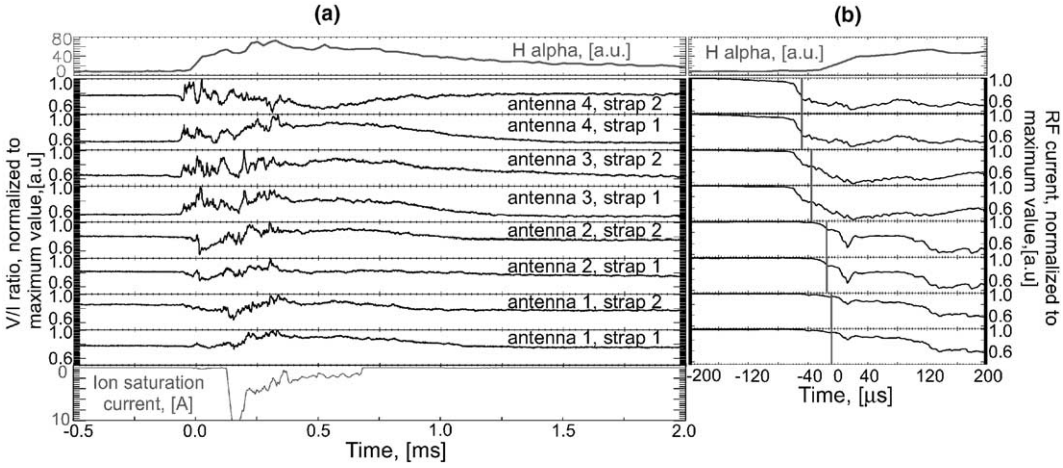

Fig. 2. (a) Time traces for H_α, V/I ratio at different antenna straps and saturation current measured by a Langmuir probe at the outer midplane. (b) Time traces for RF current. The vertical lines are the time points where the first derivative of the signal is maximal.

On the low field side at midplane, the reciprocating probe [11] has been used to measure ion saturation current. The ion saturation current to one of the probe pins is illustrated in the lower part of Fig. 2(a). Usually the response of this signal to the rising edge of an ELM comes later than the response from the antennas. This local measurement (scale of millimeters) confirms the observation of evolution of the filament-like structures during ELMs by ICRF antennas (scale of tens of centimeters) and also fits to the picture of an ELM development as an MHD instability leading to a complex pattern of power and particle deposition on the plasma facing components [12].

At the very beginning (rising edge) of ELMs, the antenna signals show that for most of the cases, ELM perturbation moves toroidally in the direction opposite to plasma current direction, i.e. in electron diamagnetic drift direction. This statement is consistent with observation of ELM-precursors and ELM activity by magnetic coils on different machines [13–15]. The best view of the propagation of ELM perturbation around torus is achieved by using the amplitudes of the RF current since these are extremely sensitive to changes of RF load during ELMs. The case considered in Fig. 2(a) is presented in Fig. 2(b) with RF current signals. An algorithm is applied using time points of the maximal first derivative of the signals, i.e. the most dynamical point of the change of the signals, to derive propagation times. The analyzed times of ELM propagation between two antenna pairs (180° in torus) for the given shot are in the range 25–150 μs. In many cases the times of propagation of ELM perturbation can be overestimated since the time evolution of the RF signals does not stay constant from strap to strap (ELM structure is strongly non-stationary at the rising edge of ELMs). Therefore minimal values from Fig. 3(b) present the cases where evolution of the ELM perturbation during toroidal propagation has little influence on the toroidal propagation times deduced from the RF signals. Minimal values result in a 50 μs time required for ELM perturbation in the taken discharge to spread around the torus (360°). This time is of the order or smaller than the parallel ion transit time, however the real nature of this propagation has not been determined yet.

The differences of the response of the antennas to ELMs have marginal effects for the design of ELM-resilient ICRF systems, if two straps or antennas used in an RF compensation scheme are located toroidally close to each other (less than 70° of toroidal angle, see also [16]).

3.3. Influence of ELMs on arcing on the antennas

To study influence of ELMs on arcing in the antennas, data was taken from ICRF minority heated discharges with type I ELMs with periods between 5 ms and 20 ms. The analysis included 102 arcs. Fig. 3(a) presents the experimental distribution of number of arcs versus time between ELM and arc. The negative times between ELMs and arcs represent the same data set with respect to the ELM which follows arc. Each point in the figure corresponds to the number of arcs counted in a 1 ms range of the delays. Since the ELM period changes over the mentioned range, the probability of arcing is biased towards the smaller values of the time between ELM and arc. In order to eliminate this bias, a probability function for ELM periods was obtained for the whole data set. Then the experimental curve in Fig. 3(a) was renormalized by dividing each point by the value of the probability function at equal values of the ELM periods and the times between ELMs and arcs.

The resulting picture is represented in Fig. 3(b). The negative delays are occasional (do not correlate with ELMs). The positive delays have two separated maxima with high number of arcs. The first one appears right after ELMs and indicates the arcs initiated during ELMs [2]. The second maximum has a delay of about 10 ms from start of ELMs. Arcs are likely to appear also with a certain delay after an ELM crashes the plasma density

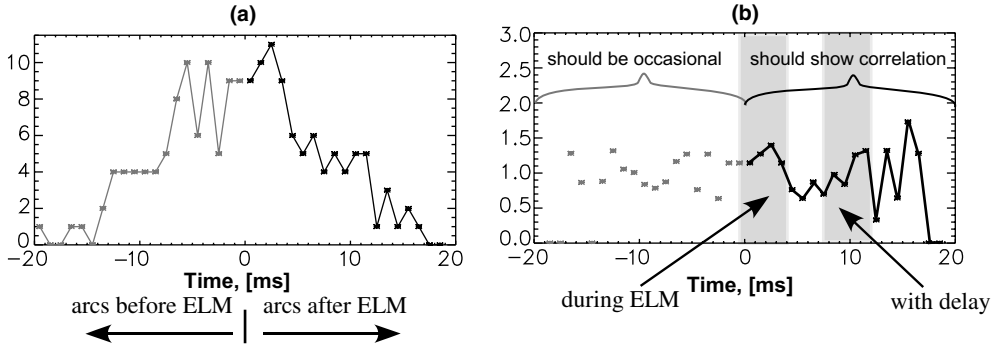

Fig. 3. (a) Initial number of arcs depending on time between ELM and arc, averaged over 1 ms. (b) Number of arcs renormalized according to the probability (see text) of occasional appearance of arcs.

profile because of the following mechanism. ELM leads to an increase of plasma density in front of the antenna and in the antenna box and to an increase of neutral gas pressure by particle induced gas desorption. The increased neutral pressure accompanied by the presence of the plasma may easily lead to the ignition of an ionization RF gas discharge and consequently to an arc. In this case it is probable that the delay between ELM and arc has a certain value due to fixed geometry of the antennas and therefore fixed neutral gas diffusion times. Often a small increase of this time delay between ELMs and arcs is observed within one AUG shot from arc to arc. Also the number of arcs initiated immediately after or during ELMs decreases from shot to shot. One can conclude that ELMs play a significant role in conditioning of the antennas. The basic mechanisms of this conditioning include bombardment of RF electrode surfaces with high energy ions, gas desorption, and surface modification processes enhanced in the presence of plasma. Thus ELMs do lead to arcing, but while doing that, participate in improving the voltage stand-off of the antennas.

4. Summary and conclusions

Observations of strong changes of coupling characteristics during ELMs in the case of the on-axis ICRF minority heating with various power in high triangularity discharges confirm the observations at JET reported in [10]. In addition, it is observed that during extreme off-axis minority heating, the changes of the antenna resistance are smaller at high triangularity.

Toroidal asymmetries of the response of ICRF antennas to ELMs are observed. Differences in times of response of toroidally distributed antennas to the rising edge of ELMs indicate a toroidal propagation of the ELM perturbation with typically a time of 50 μs required for the perturbation of the density profile to finish a single toroidal turn. The direction of propagation in most cases is observed to be counter-current, hence the perturbation of the edge plasma density follows MHD perturbation [13–15]. The differences in time of the response to the rising edge of ELMs and in the further evolution of the RF time traces on a longer time scale (up to 100–500 μs) become more pronounced for the farthest antennas. These differences will affect marginally the ELM-resilient ICRF systems as long as two antennas or straps toroidally close to each other (<70° in torus) are used.

Observations of arcing show that RF breakdown on the antennas is probable during ELMs and with a fixed delay after ELMs. From shot to shot, number of arcs during ELMs is decreased and delays between ELMs and arcs are increased. Thus ELMs often initiate arcing as well as play an important role in improving voltage stand-off of the ICRF antennas.

Acknowledgments

We are grateful to all members of ICRF team at ASDEX Upgrade, especially Mr. H. Faugel and Mr. H. Kneidl, for intensive work on the technical issues of the ICRF systems. We would like to thank Professor Dr H. Zohm, Dr T. Eich, Dr H.-W. Müller, Dr J. Neuhauser, Dr W. Suttrop and Dr A. Herrmann for helpful discussions about boundary plasma physics.

References

[1] Vl.V. Bobkov et al., in: 30th EPS Conference on Plasma Physics and Controlled Fusion, St. Petersburg, ECA Vol. 27A, 2003, P-1.165.
[2] Vl.V. Bobkov et al., J. Nucl. Mater. 313 (2003) 956.
[3] G. Bosia, Fus. Sci. Technol. 43 (2003) 153.
[4] I. Monakhov et al., in: 15th Topical Conference on Radiofrequency Power in Plasmas, Moran, AIP Conference Proceedings, vol. 694, 2003, p. 146.
[5] P.U. Lamalle et al., in: 15th Topical Conference on Radiofrequency Power in Plasmas, Moran, AIP Conference Proceedings, vol. 694, 2003, p. 118.
[6] F. Braun, F. Hofmeister, F. Wesner, W. Becker, H. Faugel, D. Hartmann, J.-M. Noterdaeme, Fus. Eng. Des. 56 (7) (2001) 551.
[7] J.-M. Noterdaeme et al., in: 21st EPS Conference on Plasma Physics and Controlled Fusion, Montpellier, ECA Vol. 18B, 1994, p. 842.
[8] J.-M. Noterdaeme et al., Fus. Eng. Des. 24 (1994) 65.
[9] H. Urano et al., Plasma Phys. Control. Fus. 45 (2003) 1571.
[10] I. Monakhov et al., in: 15th Topical Conference on Radiofrequency Power in Plasmas, Moran, AIP Conference Proceedings, vol. 694, 2003, p. 150.
[11] V. Rohde et al., J. Nucl. Mater. 241–243 (1997) 712.
[12] T. Eich, R-3, these proceedings. doi:10.1016/j.jnucmat.2004.09.051.
[13] H. Reimerdes et al., Nucl. Fus. 38 (1998) 319.
[14] T. Kass et al., Nucl. Fus. 38 (1998) 111.
[15] M. Becoulet et al., Plasma Phys. Control. Fus. 45 (2003) A93.
[16] Vl.V. Bobkov et al., in: 31st EPS Conference on Plasma Physics and Controlled Fusion, London, 2004.